Isotope Effect on Pedestal Structure in DIII-D

Ryan A Chaban[1], **S. Mordijck**[1], **T.H. Osborne** [2], **M. Knolker** [2], **K.E. Thome** [2], **F.Laggner** [3], **A.M. Rosenthal** [4]

1. *College of William & Mary, Williamsburg, Virginia, USA*
2. *General Atomics, San Diego, California, USA*
3. *Princeton Plasma Physics Laboratory, Princeton, New Jersey, USA*
4. *Massachusetts Institute of Technology, Plasma Science and Fusion Center, Cambridge, Massachusetts, USA*

Heavier hydrogenic isotopes have better confinement times and performance especially in the H-mode confinement regime. This effect manifests in significantly higher L-H transition power ($P^H_{L\to H} \gtrsim 2P^D_{L\to H}$) and lower pressure pedestals in hydrogen compared to deuterium. The isotope effect primarily comes from the edge pedestal region [1] where steep gradients interact with edge fueling and MHD peeling-ballooning stability. Many studies have investigated the isotope effect on heat transport on several machines such as ASDEX [2] and DIII-D [3]. However, the isotope effect on particle transport is more difficult to quantify due to the presence of an edge source term from fueling or divertor neutral particles ionizing inside the separatrix. Understanding the isotope effects on our models is critically important to predicting ITER PFPO 1 hydrogen operations. Extrapolating to future tokamaks such as ITER is even more difficult because their Scrape Off-Layers (SOL) are hot and dense enough to eliminate fueling inside the separatrix.

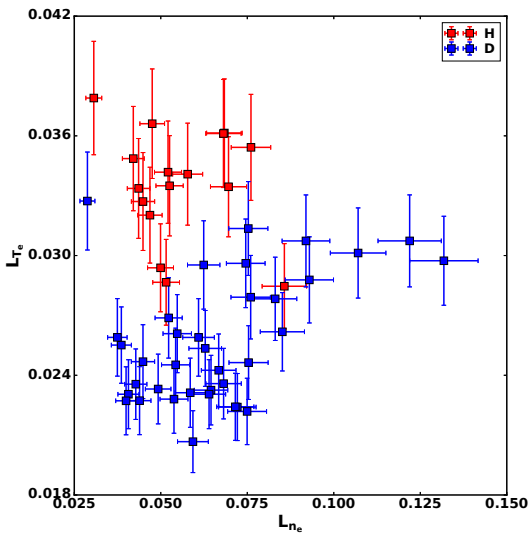

Fig. 1 Temperature gradient scale length vs. density gradient scale length for hydrogen(red) and deuterium (blue). Scale lengths are measured in meters along the vertical Thomson Scattering chord.

In this study we examine whether there exist systematic pedestal structure differences between hydrogen and deuterium in stationary (>500ms) H-modes on DIII-D and investigate whether those differences are more likely caused by fueling or transport. We use a dataset of hydrogen and deuterium, which consists of 36 deuterium discharges and 16 hydrogen discharges from an experiment attempting to recreate the core and edge conditions of the deuterium experiment. All discharges are lower single null with similar triangularity, a range of collisionalities ($\nu^* \sim 0.1-5$), I_p / B_T, and input powers ranging from 3-8MW varying the Electron Cyclotron Heating (ECH) and Neutral Beam Injection (NBI) mixture. In this analysis, stability changes from shaping are relatively minor; however, it is clear that particle transport is different in ECH+NBI discharges compared to NBI only discharges.

To examine the effects of transport, we examine the normalized edge electron density and temperature gradients ($L_x = x/\nabla x$) and the ratio of these gradients $\eta_e \equiv L_{n_e}/L_{T_e}$ averaged over the steep gradient region ($0.95 \lesssim \psi_n < 1.0$). Simulation work on DIII-D has shown that η_e exhibits a critical threshold behavior where Electron Temperature Gradient (ETG) microturbulence increases significantly when $\eta_e \gtrsim 1.4$ [4]. The average gradients and resulting scale lengths are approximated using the height and width of an edge hyperbolic tangent fit to the Thomson Scattering averaged over a stationary state (>500ms). Figure 1 shows the temperature

and density gradient scale lengths for both isotopes. There is a clear separation by isotope in the temperature channel while the range in L_{n_e} for each isotope overlap. The larger edge temperature gradients scale lengths shown for hydrogen in figure 1 are a consequence of the increased heat transport in hydrogen. These scale lengths are larger despite the average heating power in the hydrogen discharges being $\sim$ 20% higher to maintain a stable H-mode. However, the density gradient scale lengths overlap. This indicates that the isotope effect affects the the particle and heat transport channels separately and while there is clearly increased heat transport, much more investigation is required to understand the particle transport.

Direct quantification of the edge source term is difficult. Empirically, more fueling increases the separatrix density, while increasing the pedestal density less and increasing the ratio of separatrix density over pedestal density (n_e^{SEP}/n_e^{PED}) [5]. The data show that the density pedestal (steep gradient region) is "shifting" outwards with respect to the temperature pedestal and this behaviour has been observed on DIII-D, JET, and ASDEX [6]. This rise in n_e^{SEP} also decreases ballooning stability, while the shift increases η_e and moves the bootstrap current outwards affecting the peeling stability [6]; however, these effects are outside the scope of this conference paper.

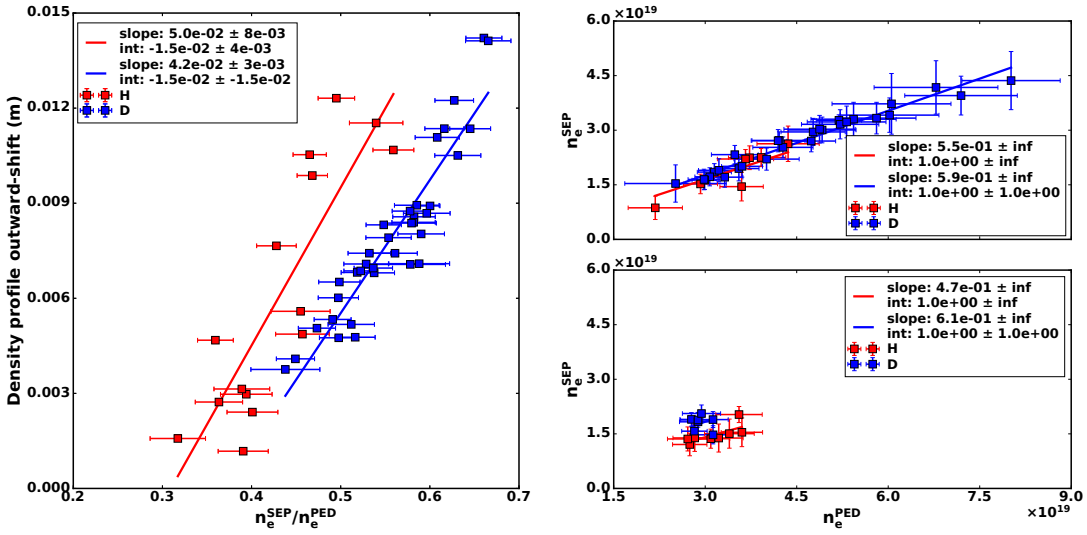

Fig. 2 (left) profile shift (steepest point of each profile as defined by the tanh-symmetry point: $n_e^{SYM} - T_e^{SYM}$) vs. n_e^{SEP}/n_e^{PED}. (right) $n_e^{SEP} vs. n_e^{PED}$ for NBI only (top row) and ECH+NBI (bottom row).

Figure 2 (left) shows the profile shift as a function of the ratio n_e^{SEP}/n_e^{PED}. The slope of the shift is similar for each isotope most likely since the profiles are following the same functional form of a hyperbolic tangent function. The x-intercept indicates a systematic difference where hydrogen pedestals tend to have lower n_e^{SEP}/n_e^{PED} compared to deuterium. The range of the hydrogen data also extends to lower n_e^{SEP}/n_e^{PED} and the range of deuterium increases past hydrogen. Hydrogen neutrals have a $\sqrt{2}$ faster velocity and this increased penetration could be contributing to the slight decrease in the ratio of n_e^{SEP}/n_e^{PED} . However the decrease is on the order of 12% and cannot fully explain the isotope effect.

Figure 2 (right) examines the isotope difference for n_e^{SEP}/n_e^{PED} separating the data by heating power. The NBI-only discharges (top row) indicate a similar ratio although the range of hydrogen data is limited in pedestal height. For discharges with NBI+ECH heating (bottom) the slopes

are within error; however, there is significant scatter and this dataset only consists of a small range of n_e^{SEP} and n_e^{PED}. Future work will investigate whether ECH pumpout is altered by the isotope effect. Overall the data are suggestive of a small dependence on fueling as the primary contributor to the pedestal structure difference from the isotope effect.

We also examine the effects of the ratio of n_e^{SEP}/n_e^{PED} on the gradient scale lengths. Figure 3(top) shows that the density scale length responds differently between isotopes. Hydrogen tends to have narrower (lower L_{n_e}) pedestals that widen more slowly with increased n_e^{SEP}/n_e^{PED} than deuterium pedestals indicated by the decreased slope. By demonstrating earlier that fueling is not especially different between the isotopes, this is most likely a result of a change in particle transport. However, increased particle diffusivity would smooth out and widen the hydrogen pedestals; therefore, this might demonstrate a difference in a convective pinch term between the isotopes.

Figure 3 (bottom) shows that hydrogen L_{Te} decreases as the ratio of n_e^{SEP}/n_e^{PED} is increased while for deuterium L_{Te} *increases*. However, this effect is less significant than it appears at face value. The separatrix temperature in DIII-D is generally fixed between 70-100eV due to power balance using the two-point SOL [7]. However, our dataset currently uses an automated hyperbolic tangent fitting algorithm and the separatrix temperature and pedestal temperature each vary by a factor of 5 while the ratio of T_e^{SEP}/T_e^{PED} only varies between 0.26-0.32. Overall the magnitude of L_{T_e} only varies by a factor of two from the highest hydrogen discharge to the lowest deuterium discharge and is caused by the increased heat transport in hydrogen mentioned previously. What may be interesting for future detailed analysis is inspecting the discharges with similar L_{T_e} at higher at $n_e^{SEP}/n_e^{PED} = 0.5$.

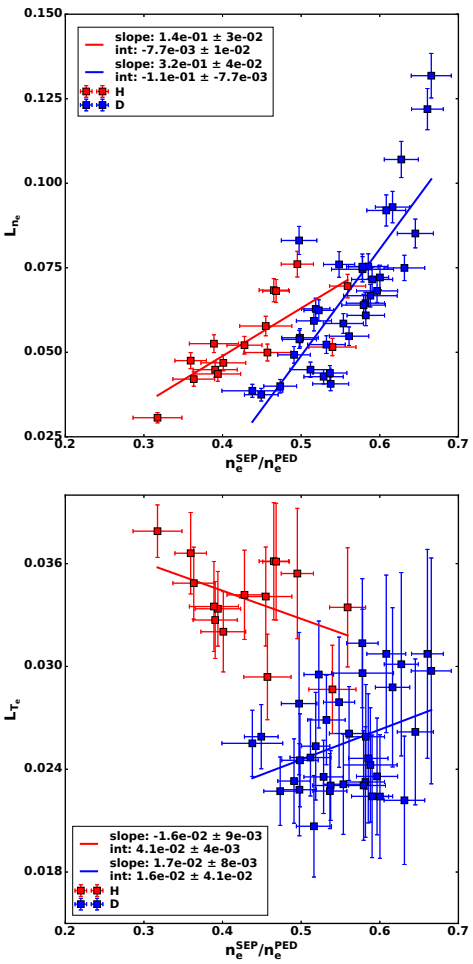

Fig. 3 (top) L_{ne} vs. n_e^{SEP}/n_e^{PED} . (bottom) L_{Te} vs. n_e^{SEP}/n_e^{PED} .

Another method of analyzing the the isotope effect on transport vs.fueling is to examine the ELM dynamics. Type-I ELMs are defined by increasing frequency with increasing injected power and this is true within our dataset. Figure 4 (left) shows there is not much of a correlation between ELM frequency and n_e^{SEP}/n_e^{PED} other than the difference in n_e^{SEP}/n_e^{PED} between hydrogen and deuterium previously described. The ELM frequency does not have any clear dependence on T_e, ∇T_e, n_e, or ∇n_e.

ELM frequency is also known to change with respect to the location of the pedestal on the peeling-ballooning stability diagram. Preliminary work has shown that hydrogen discharges are more often ballooning (pressure) limited rather than peeling (current) limited. This is true especially in comparison to deuterium discharges at matched injected power and q_{95} because the

increased heat transport means that lower pressure gradients will drive less bootstrap current. Figure 4 (right) shows ELM frequency vs. η_e and the steeper slope of hydrogen might represent a limit of ballooning ELMs, while the scatter in deuterium could be explained by being located at different positions on the peeling ballooning stability diagram with larger slower ELMs. Future work in this area will investigate the role of T_e/T_i for driving the transport and ELM frequency for ECH+NBI vs. NBI-only heated plasmas in hydrogen and deuterium.

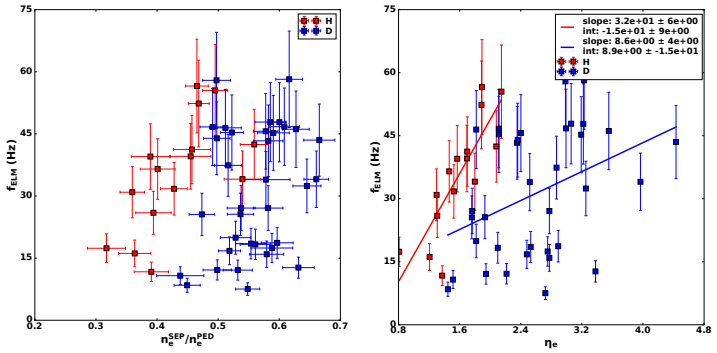

Fig. 4 (left) ELM frequency vs. n_e^{SEP}/n_e^{PED} and (right) ELM frequency vs. η_e.

Using a dataset of hydrogen and deuterium discharges on DIII-D we investigate the isotope effect primarily in the particle channel, and whether the driving factors are fueling or transport. The ratio of n_e^{SEP}/n_e^{PED} changes consistently for both isotopes but is slightly lower for hydrogen discharges. The changes from increasing n_e^{SEP}/n_e^{PED} on L_{n_e} are less pronounced in hydrogen, suggesting there may be a difference in convective pinch between the isotopes, and there are almost no changes in L_{T_e}. For ELMs, other than the shift to lower n_e^{SEP}/n_e^{PED} for hydrogen, there is no difference in the frequency; yet there is a clear dependence on η_e. All of these factors suggest that hydrogen pedestal structure is more strongly influenced by transport with a small contribution from fueling.

Future work will use the calibrated Lyman-α LLAMA diagnostic [8] to infer neutral ionization profiles and quantify the fueling of deuterium and hydrogen discharges on DIII-D. We will also make use of the turbulence diagnostics to examine hydrogen and deuterium pedestal density and temperature height matches to measure the dominant type of microturbulence. Combining this information with the profiles will allow a direct comparison of the isotope effect on fueling versus transport in setting the pedestal.

Acknowledgement: This material is based upon work supported by the U.S. Department of Energy, Office of Science, Office of Fusion Energy Sciences, using the DIII-D National Fusion Facility, a DOE Office of Science user facility, under Award(s) DE-FC02-04ER54698 and DE-SC0019302.

References

[1] E. Belli et al. Physical Review Letters, **125**, 1, (2020)
[2] P. Schneider et al. Plasma Physics and Controlled Fusion, **63**, 6, (2021)
[3] E. Belli et al. Physics of Plasmas, **26**, 8, (2019)
[4] W. Guttenfelder, Nuclear Fusion, **61**, 5, (2021)
[5] S. Mordijck, Nuclear Fusion, **60**, 8, (2020)
[6] L. Frassinetti et al. Nuclear Fusion, **59**, 7, (2017)
[7] A. W. Leonard et al. Nuclear Fusion, **57**, 086033, (2021)
[8] A.M. Rosenthal, Review of Scientific Instruments, **92**, 3, (2021)